



# Optimization on thermal treatment synthesis of lactoferrin nanoparticles via Taguchi design method

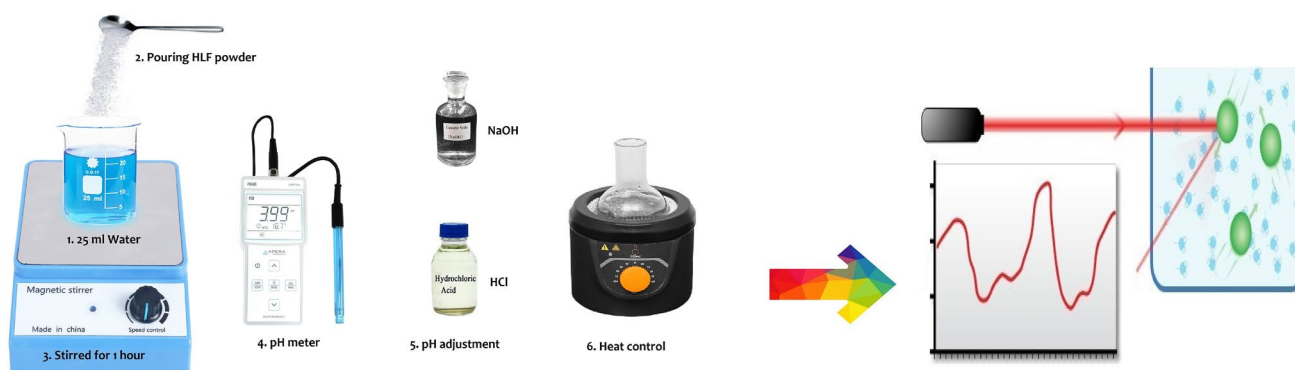
Roozbeh Mofidian<sup>1,2</sup> · Abolfazl Barati<sup>1</sup> · Mohsen Jahanshahi<sup>2</sup> · Mohammad Hassan Shahavi<sup>3</sup>

© Springer Nature Switzerland AG 2019

## Abstract

Lactoferrin is a globular protein-based biopolymer which has many applications in pharmacy and food industry. In this study, human lactoferrin nanoparticles were synthesized by thermal treatment technique. Taguchi array design was employed to minimize the size of nanoparticles. To gain as this purpose, four main factors with four different levels involved as: lactoferrin concentration (1–4 mg/mL), pH values (6–9), heating rate of (2–5 °C/min) and final temperature of (60–90 °C) were investigated. In the following, prepared nanoparticles were characterized by dynamic light scattering, Fourier transform infrared spectroscopy, scanning electron microscopy, and atomic force microscopy analysis. Analysis of variance showed that lactoferrin concentration with the contribution percentage of 45% is most important in the preparation of nanoparticles. Also, optimal conditions for synthesized nanoparticles by thermal treatment technique were: LF concentration of 3 mg/mL, pH 8, heating rate of 3 °C/min and final temperature of 90 °C to achieve particle size of 188.8 nm, polydispersity index of 0.317 and zeta potential of – 52.2 mV.

## Graphic abstract

**Keywords** Lactoferrin · Nanoparticles · Optimization · Particle size · Taguchi design

✉ Mohammad Hassan Shahavi, m.shahavi@ausmt.ac.ir | <sup>1</sup>Department of Chemical Engineering, Faculty of Engineering, Arak University, Arāk, Iran. <sup>2</sup>Nanotechnology Research Institute, Babol Noshirvani University of Technology, Babol, Iran. <sup>3</sup>Faculty of Engineering Modern Technologies, Amol University of Special Modern Technologies (AUSMT), Amol, Iran.

SN Applied Sciences (2019) 1:1339 | <https://doi.org/10.1007/s42452-019-1353-z>

Received: 31 July 2019 / Accepted: 24 September 2019 / Published online: 5 October 2019

## 1 Introduction

According to WHO statistics, less than 20% of preschool children in developed countries and about 50% in developing countries have iron deficiency [1]. Scientists in medicine and chemistry believe that lactoferrin (LF) can solve many health problems of iron deficiency. Therefore, researchers have tried to use LF to transfer iron to the cells and control the level of free iron in the blood and external secretions [2].

The two main types of LF include human LF (HLF), and bovine LF (BLF) [3]. Milk is a rich source of LF. The levels of LF in normal milk vary considerably between species. Colostrum is the first form of milk produced by mammals immediately after birth, containing large amounts of LF [4]. Considering the importance of LF and its global demands, the production of recombinant LF has become the main goal for chemical engineers. It seems that the main physiological function of LF is to bind iron. Hence, LF helps regulate the absorption of iron in the intestine and delivery of iron to the cells. The antimicrobial activity of LF is related to bacterial lysis or opsonization of the pathogen, for example, mannose-binding proteins' interaction with HIV and neutralization of influenza A virus by surfactant protein A [5]. The chemical structure of pure LF is shown in Fig. 1. It consists of a single-chain polypeptide with two globular lobes which further contain two major domains that are responsible to serve as the binding and glycosylation sites for iron molecules and carbonate ions.

Recently, there is also a growing interest in the potential use of LF for the improvement of bone health and cancer prevention [6, 7]. Further, the exciting potentials of employing nanotechnology in advancing drug delivery systems, active disease targeting and prognosis have also

shown some encouraging outcomes. The mechanisms by which lactoferrin develops antibacterial activity, depend on the type of microorganism. LF could be considered an ideal nutraceutical product because of its relatively cheap production from bovine milk and of its widely recognized tolerance after ingestion, along with its well-demonstrated protective activities [8]. LF influences the growth and proliferation of a diversity of bacteria such as Gram-positive and Gram-negative bacteria. However, LF has constructive effects on lactobacillus and bifidobacterium growth [9]. LF consumption might protect the host from viral infections through inhibiting the attachment of a virus to the cells, replication of the virus in the cells, and enhancement of systemic immune functions. LF were successfully immobilized on glass surfaces and showed promising antimicrobial activity against pathogenic bacteria [10].

Investigation of growth mechanism of nanoparticles (NPs) is present large scientific and practical interest [11–13]. Utilizing LF by combining its multifunctional properties with nanotechnology can be a remarkable therapeutic agent [14]. Several approaches are available to synthesized LF-NPs including thermal treatment, phase separation, emulsion templating, and adsorption methods [15]. Also, understanding the bioactive compound release mechanisms is essential for predicting the behavior of lactoferrin nanoparticles during food production or food consumption. Due to the importance of LF, research into the purification and optimization of LF-NPs synthesis is increasing continually. LF is an excellent NPs carrier because it is non-toxic and non-immunogenic. Moreover, LF-NPs are not required to form polymeric materials or surfactants [16].

Taguchi method is a reliable and suitable method for optimization of nanobio-products [17–19]. In this research, Taguchi design experiment software was used to optimize the size of LF-NPs by thermal treatment method. As mentioned above, four main factors in four levels considered: LF concentration (1–4 mg/mL), pH (6–9), heating rate (2–5 °C/min), and final temperature (60–90 °C). The design of experiments was performed using MINITAB® statistical software (version 18). The analysis of variance (ANOVA) was used to obtain the best formulation for the synthesis of NPs. Finally, 16 separate experiments were prepared and the results were investigated by responses.

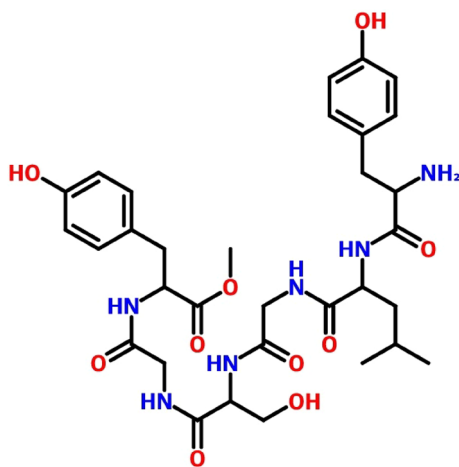


Fig. 1 Chemical structure of pure LF

## 2 Experimental

### 2.1 Materials

Purified LF powder was purchased from Merck (Darmstadt, Germany). According to data extracted from pure packaging, it contains 95% protein, 0.5% ashes, 3% moisture,

and the rest of iron. Hydrochloric acid 1 M (HCl, 37%) and sodium hydroxide 1 M (NaOH, 97%) were obtained from Sigma Aldrich Chemical Co. Ltd. (St. Louis, MO, USA).

### 2.2 Taguchi design

Today Taguchi is used as a successful model for designing experiments. In addition to the simplicity and ease of access, this software reduces the number of experiments, making research more cost-effective and economical [17, 20]. The factors and levels examined are listed in Table 1.

In fact, calculation of the degree of freedom (DF) is very important because it allows us to know how much the final calculation values are allowed to be. Clearly, the DF must be smaller (or equal) than the total number of experiments. In this work, DF equal to 15. Therefore, only 16 experiments are required to study the entire parameter space using L16 orthogonal arrays (OA). Taguchi design is based on signal, noise and control factors. The analysis is carried out using Signal to Noise Ratio (SNR) for Higher the Better (HB) criteria using the formula as given below.

$$\frac{S}{N_{HB}} = -10 \log \left[ \frac{1}{k_i} \sum_{i=1}^k \frac{1}{y_i^2} \right] \tag{1}$$

where  $N_{HB}$  is the number of HB criteria,  $n$  is total number of trial runs at  $i$ th setting,  $y_i$  is value of the response at  $i$ th setting and  $k$  is the total number of replications. The SNR can analyze and identify the factor that significantly affects the output, as well as the amount of the contribution of each factor. Further, relative effect of each process parameter is determined by the Analysis of Variance (ANOVA) which is a statistical technique. In this technique the total variability of the response is separated with respect to individual contributions of each of the factors and the error. To determine the contribution of each parameter, the contribution percentage that is described as follows, needs to be calculated for each parameter.

$$\%Contribution = \frac{SS}{SS_{tot}} \times 100 \tag{2}$$

where  $SS$  is the sum of squares and  $SS_{tot}$  is the total sum of squares. Since the main purpose of this study is to reduce the size of LF-NPs, the increase of the contribution

percentage indicates the importance of that parameter in achieving the desired target. Table 2 shows the experimental design of Taguchi method.

### 2.3 ANOVA

ANOVA is a statistical tool in Taguchi software that analyzes the results of each parameter relative to overall changes. The one-way ANOVA is used to determine whether there are any statistically significant differences between the means of three or more independent groups. Calculation of the standard terms involved in ANOVA table such as the sum of squares (SS) that given in Eq. (3):

$$SS_p = \frac{SN_1}{N_1} + \frac{SN_2}{N_2} + \frac{SN_3}{N_3} + \frac{SN_4}{N_4} \tag{3}$$

The sum of squares is a measure of deviation from the mean. The term  $SS_p$  refers to the sum of squares and indices  $p$  due to parameter  $P$ . For example,  $SN_1$  is the sum of

**Table 2** Experimental design of Taguchi; A: LF concentration (mg/mL), B: pH, C: heating rate (°C/min), D: final temperature (°C)

| Run | Process parameter            |            |                           |                            |
|-----|------------------------------|------------|---------------------------|----------------------------|
|     | (A) LF concentration (mg/mL) | (B) pH (-) | (C) Heating rate (°C/min) | (D) Final temperature (°C) |
| 1   | 1                            | 5          | 1                         | 60                         |
| 2   | 1                            | 6          | 2                         | 70                         |
| 3   | 1                            | 7          | 3                         | 80                         |
| 4   | 1                            | 8          | 4                         | 90                         |
| 5   | 2                            | 5          | 2                         | 80                         |
| 6   | 2                            | 6          | 1                         | 90                         |
| 7   | 2                            | 7          | 4                         | 60                         |
| 8   | 2                            | 8          | 3                         | 70                         |
| 9   | 3                            | 5          | 3                         | 90                         |
| 10  | 3                            | 6          | 4                         | 80                         |
| 11  | 3                            | 7          | 1                         | 70                         |
| 12  | 3                            | 8          | 2                         | 60                         |
| 13  | 4                            | 5          | 4                         | 70                         |
| 14  | 4                            | 6          | 3                         | 60                         |
| 15  | 4                            | 7          | 2                         | 90                         |
| 16  | 4                            | 8          | 1                         | 80                         |

**Table 1** Factors and levels of experiments

| Factors/levels    | Units    | Symbols | 1  | 2  | 3  | 4  |
|-------------------|----------|---------|----|----|----|----|
| LF concentration  | (mg/mL)  | A       | 1  | 2  | 3  | 4  |
| pH                | -        | B       | 5  | 6  | 7  | 8  |
| Heating rate      | (°C/min) | C       | 1  | 2  | 3  | 4  |
| Final temperature | (°C)     | D       | 60 | 70 | 80 | 90 |

SNR of experiments involving parameter P at level 1.  $N_1$  is the number of experiments containing parameter P at level 1.

$$V_p = \frac{SS_p}{DF_p} \tag{4}$$

$V_p$  is the variance of parameter P.  $DF_p$  is the degree of freedom associated with parameter P. The statistical formula to determine degrees of freedom is quite simple.

### 3 Methods

#### 3.1 Synthesis of LF-NPs

LF-NPs preparation was based in the methodology used by other authors with some modifications [21]. The schematic illustration of the various steps in the production of LF-NPs with full specifications showed in Fig. 2. In this work, for preparation of LF-NPs, based on Table 2, purified LF powder with different doses (1, 2, 3 and 4 mg/mL) poured into 25 mL of distilled water and was stirred 1 h at room temperature. Then, LF solution was adjusted to different values of pH (6, 7, 8 and 9) with 1 M HCl and/or 1 M NaOH when necessary. Meanwhile, LF solution was heated slowly at a constant rate (2, 3, 4 and 5 °C/min) to the required temperature (60, 70, 80 and 90 °C). The solution was filled into serum vials, and the vials were placed directly on the shelves of the freeze-dryer (TFD 5505, IL shin Bio-Base Ltd., South Korea). Synthesized LF-NPs was stored in a refrigerator at a temperature of 4 °C. Figure 3 shows LF-NPs after freeze drying.

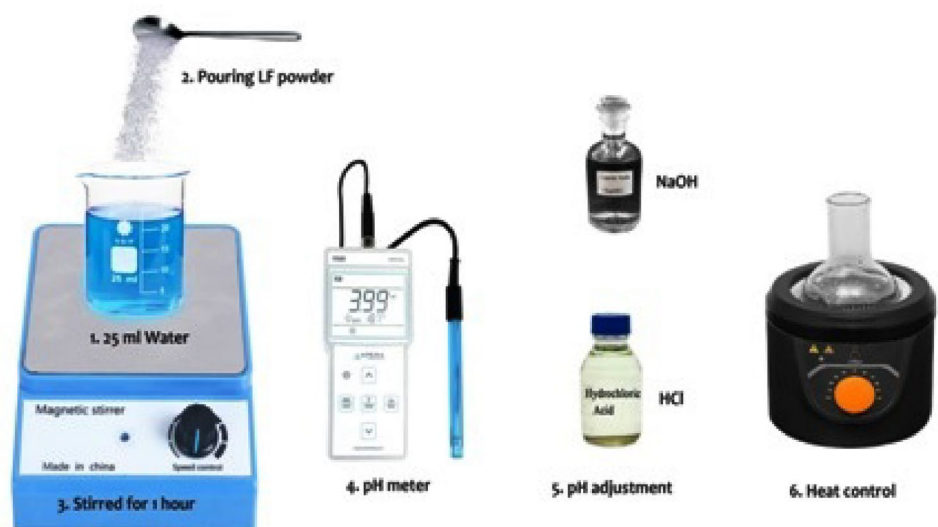


Fig. 3 The final product of solid LF-NPs

#### 3.2 Particle size and polydispersity index analysis

The size of the NPs can be determined by measuring random variations in the dispersion of light from a suspension or dilute solution. This method is referred to as dynamic light scattering (DLS), Photon correlation spectroscopy and also called quasi-elastic light scattering [22]. Particle sizes and polydispersity index (PDI) of biopolymer particles were determined using a modern known device yclept as DLS or particle size analyzer (Malvern Mastersizer Instruments, UK). The results of DLS analysis include two independent parameters: Z-average mean diameter and PDI. PDI is used to estimate the average uniformity of a particle solution, and bigger PDI values correspond to a larger size distribution in the particle sample.

Fig. 2 Schematic view of the progressive steps in preparation of LF-NPs solution



### 3.3 Fourier transforms infrared spectroscopy analysis

Fourier transform infrared (FTIR) spectroscopy is an analytical technique used to identify organic, polymeric, and, in some cases, inorganic materials. The FTIR analysis method uses infrared light to scan test samples and observe chemical properties. The basic theory at work is that the bonds between different elements absorb light at different frequencies. In this work, FTIR analyses were conducted to interact between LF-NPs and pure LF. FTIR spectroscopy was taken on Rayleigh (model WQF-510A from China).

### 3.4 Scanning electron microscopy

Scanning electron microscopy (SEM) analysis is an authoritative analytical apparatus which uses a focused beam of electrons to fabricate complex, elevated magnification photos of a sample [23]. Briefly, NPs were coated via a gold sputter coater and observed by SEM (SNE-4500M, SEC Cooperation, Suwon. Ltd., South Korea) working at 20 kV in high vacuumed condition.

### 3.5 Atomic force microscopy

Atomic force microscopy (AFM) can appraise changeable NPs geometry, from traditional spherical NPs to more interesting fractal geometries of NPs. In this study, AFM analysis was executed by EasySacr II<sup>®</sup> (Nanosurf, Liestal, Switzerland). Data acquisition was performed manually using Nanosurf Data Processing software.

## 4 Results and discussion

### 4.1 Taguchi design consequences

According to Taguchi method, results of 16 experiments were tabulated in Table 3. The effects of each factor level on the quality characteristics were analyzed using the SNR. The average SNR for every level of experiment is calculated based on the recorded value as shown in Table 3. The SNR graphic of these levels were used for the evaluation (Fig. 4). The higher SNR value means better product quality. Accordingly, the contribution of each parameter determined by the method of variance and ultimately analyzed from the statistical viewpoint. Furthermore, the curve observation showed that the 'A' factor (LF concentration) most influences the particle size. It means that the change in concentration of LF is a fundamental factor. On the contrary, the lowest effect on particle size is final temperature. For the present experimental condition the best suitable design is Taguchi's L16 OA which is shown in Table 3.

As shown in Table 4, the direct effect of each parameter at the desired level was investigated using means analysis and its response mentioned as delta parameter. The ranks and the delta values for various parameters show that LF concentration has the greatest effect on particle size and is followed by heating rate, pH and final temperature in that order.

To use the F-test to determine whether group means are equal, it's just a matter of including the correct

**Table 3** Experimental design with results

| Specimen | Process parameter    |        |                  |                       | Size (nm) | PDI   |
|----------|----------------------|--------|------------------|-----------------------|-----------|-------|
|          | (A) LF concentration | (B) pH | (C) Heating rate | (D) Final temperature |           |       |
| 1        | 1                    | 1      | 1                | 1                     | 503.3     | 0.509 |
| 2        | 1                    | 2      | 2                | 2                     | 685.3     | 0.703 |
| 3        | 1                    | 3      | 3                | 3                     | 363.7     | 0.42  |
| 4        | 1                    | 4      | 4                | 4                     | 665.2     | 0.593 |
| 5        | 2                    | 1      | 2                | 3                     | 921.6     | 0.674 |
| 6        | 2                    | 2      | 1                | 4                     | 1708      | 0.971 |
| 7        | 2                    | 3      | 4                | 1                     | 1095      | 0.706 |
| 8        | 2                    | 4      | 3                | 2                     | 650.9     | 0.567 |
| 9        | 3                    | 1      | 3                | 4                     | 163.5     | 0.259 |
| 10       | 3                    | 2      | 4                | 3                     | 282.5     | 0.337 |
| 11       | 3                    | 3      | 1                | 2                     | 270.4     | 0.477 |
| 12       | 3                    | 4      | 2                | 1                     | 181       | 0.38  |
| 13       | 4                    | 1      | 4                | 2                     | 494       | 0.495 |
| 14       | 4                    | 2      | 3                | 1                     | 854.2     | 0.728 |
| 15       | 4                    | 3      | 2                | 4                     | 312.7     | 0.422 |
| 16       | 4                    | 4      | 1                | 3                     | 1863      | 0.84  |



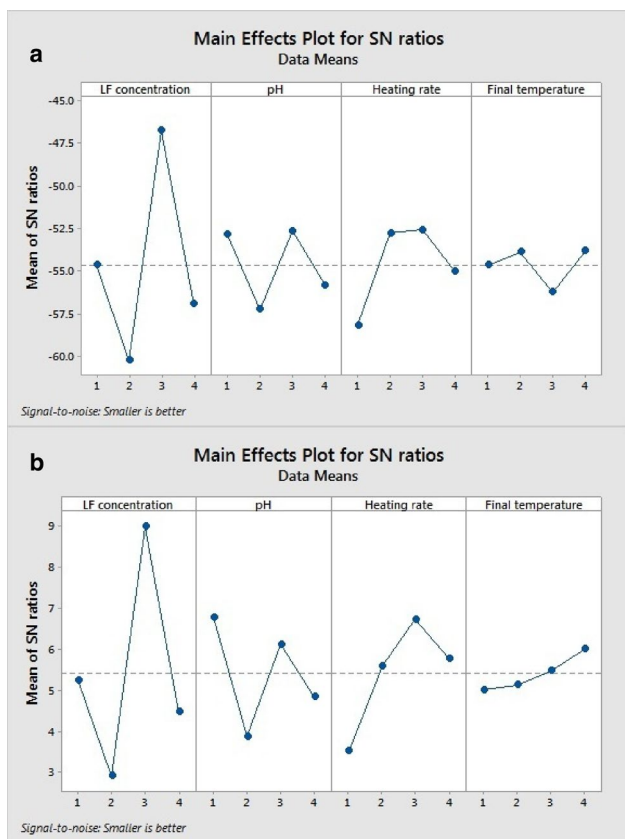


**Fig. 4** Analysis of SNR graph by **a** size and **b** PDI versus A (LF concentration), B (pH), C (heating rate), D (final temperature) factors

**Table 4** Response table for means

| Level | LF concentration | pH     | Heating rate | Final temperature |
|-------|------------------|--------|--------------|-------------------|
| 1     | 0.5562           | 0.4843 | 0.6992       | 0.5807            |
| 2     | 0.7295           | 0.6847 | 0.5448       | 0.5605            |
| 3     | 0.3632           | 0.5062 | 0.4935       | 0.5677            |
| 4     | 0.6212           | 0.5950 | 0.5327       | 0.5613            |
| Delta | 0.3663           | 0.2005 | 0.2057       | 0.0202            |
| Rank  | 1                | 3      | 2            | 4                 |

**Table 5** ANOVA for means

| Source         | DF | Seq SS  | Adj MS  | Variance  | F-value | p value | % Contribution |
|----------------|----|---------|---------|-----------|---------|---------|----------------|
| A              | 3  | 435,145 | 145,048 | 145,048.3 | 3.28    | 0.017   | 45             |
| B              | 3  | 120,592 | 40,197  | 40,197.3  | 0.91    | 0.030   | 12             |
| C              | 3  | 220,476 | 73,492  | 73,492    | 1.66    | 0.034   | 23             |
| D              | 3  | 56,789  | 18,930  | 18,929.7  | 0.43    | 0.048   | 6              |
| Residual error | 3  | 132,552 | 44,184  | 44,184    |         |         | 14             |
| Total          | 15 | 965,554 |         |           |         |         | 100            |

variances in the ratio. In one-way ANOVA, the F-statistic is described by Eq. (5):

$$F = \frac{\text{variation between sample means}}{\text{variation within the samples}} \quad (5)$$

The best way to understand this ratio is to walk through a one-way ANOVA example. The *F*-value shows the importance of a controlling factor over the quality attribute, which is the particle size in this operating system. The *F*-value for each control factor is the ratio of the mean deviations to the mean square error. The appropriate analysis on the ANOVA is centered on the mean performance characteristics and estimated by the Fischer test value (*F*-value). Usually, if *F*-value is greater than 4, it means that the control factor has a huge impact on the quality attribute. From Table 5, it can be showed that the *F*-value for LF concentration with the value of 3.28 is higher than others and is more effective than other results. The solvent heating rate also plays a serious role in the size of the LF-NPs, with an *F*-value of equal to 1.66. The *p* value explains the probability of obtaining the *F*-value of this order due to noise, and the values below 0.05 confirm the correctness of the process parameter. Based on Table 5, the concentration of LF is found to be the most impressive parameter by contributing factor 45%.

## 4.2 Optimization and confirmation

In the final step of Taguchi method, optimization is verified by confirmation experiments after the determination of the variable levels that will give the optimal results. The confirmation experiment results performed at the optimum variable levels for particle size and PDI. As determined in Fig. 4, A3B3C3D4 and A3B1C3D4 and their levels were used for the calculation of the predicted optimal particle size and PDI respectively. According to Taguchi method, the optimal levels of control factors for the size of LF-NPs are given in Table 6. As shown in Table 6, a combination of favorable conditions not found in experimental arrays achieved with the Taguchi optimization method. Therefore, for Taguchi validation, optimal results were performed again in the laboratory.

**Table 6** Optimal conditions and laboratory results

| Investigating parameters   | (a) Particle size (nm) |       | (b) PDI |       |
|----------------------------|------------------------|-------|---------|-------|
|                            | Level                  | Value | Level   | Value |
| LF concentration (mg/mL)   | 3                      | 3     | 3       | 3     |
| pH                         | 3                      | 8     | 1       | 6     |
| Heating rate (°C/min)      | 3                      | 3     | 3       | 3     |
| Final temperature (°C)     | 4                      | 90    | 4       | 90    |
| Expected result at optimum | 224.2                  |       | 0.473   |       |
| Result at laboratory       | 188.8                  |       | 0.317   |       |
| % Error                    | 15.7                   |       | 32.9    |       |

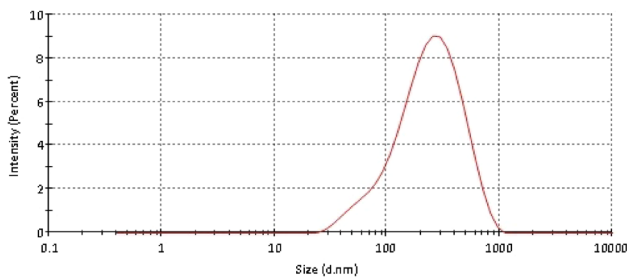


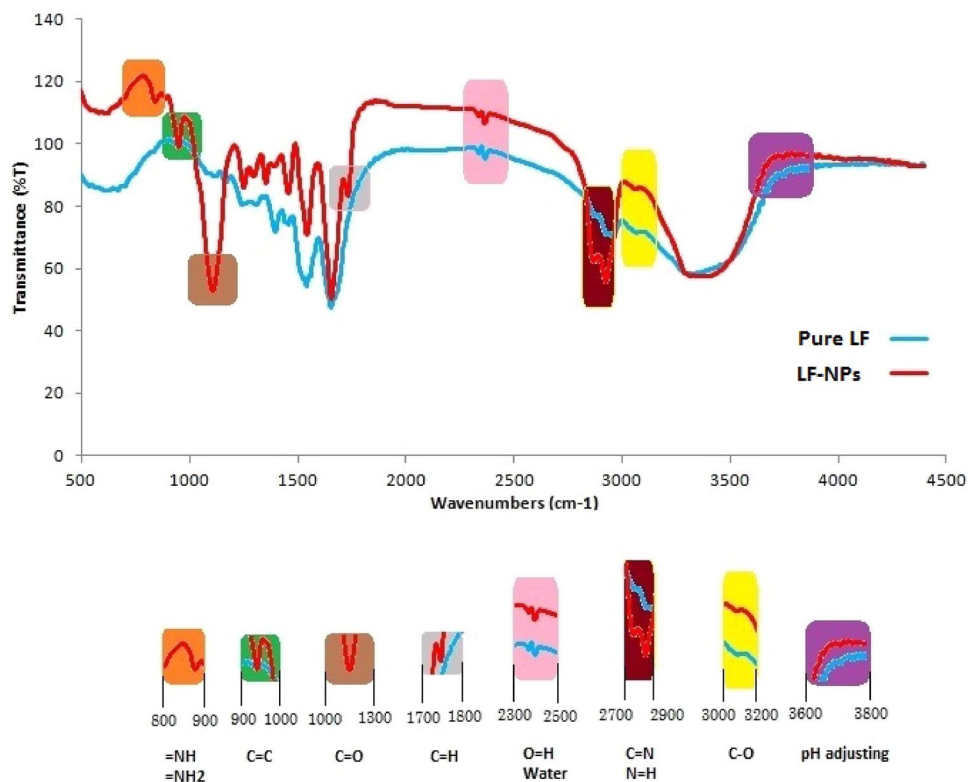
**Fig. 5** Size distribution intensity

Therefore, relying on optimized results, the experiment was restarted under optimal conditions. As clear, the predicted values by Taguchi are in close agreement with what extracted from empirical data. Presumably, in Taguchi’s design, the error rate is due to machine error in calculating particle size or due to human error [24]. The size of LF-NPs after optimization is equal to 188.8 nm, which is less than the size expected from the Taguchi method (Fig. 5).

**4.3 FTIR characterization**

FTIR analytical applications have allowed the structural characterization of biological material such as proteins. FTIR spectra of proteins are highly complex and therefore can be difficult to interpret. The FTIR spectra were recorded in the 500–4500  $\text{cm}^{-1}$  range at room temperature [25]. As shown in Fig. 6, FTIR spectra of two different samples depicted (LF-NPs and pure LF). It is shown in the graph; after the formation of the NPs, a significant decrease occurs in the intensity of the curve in 600–3600  $\text{cm}^{-1}$  region. However, pure LF does not change much, but slight changes occur in the LF curve. A weakening of peak intensities in the regions around 3800 and 3600  $\text{cm}^{-1}$ , respectively observed, which caused by a molecular interaction between LF and HCl/NaOH for adjusting pH [26]. However, significant changes were observed in the FTIR LF-NPs pattern, which is probably due to the addition of HCl or NaOH. LF-NPs reacts to protein adsorption and

**Fig. 6** FTIR spectrum of pure LF and LF-NPs



produces tensile vibrations at the intensity of  $3000\text{ cm}^{-1}$  due to C–O and  $2900\text{ cm}^{-1}$  due to N=H bending with the contribution of C=N stretching vibrations [27]. The strong band at  $2400\text{ cm}^{-1}$  is based on the tensile vibration of O=H and states that there is still some water in the sample. In the range  $1733\text{ cm}^{-1}$ , several bands are related to the tensile vibration C=H and are related to the symmetric and asymmetric traction in the  $\text{CH}_2$  and  $\text{CH}_3$  groups. The deep drop in the strip at a distance of  $900\text{--}1200\text{ cm}^{-1}$  shows the effect of the interaction between C=C and C=O in LF deformation, respectively. Also, the presence of water in the LF-NPs leads to an increase in peak intensity and changes in the region from  $\sim 1200$  to  $900\text{ cm}^{-1}$  and about the broad peak near  $\sim 3450\text{ cm}^{-1}$ . The band between  $800\text{--}600\text{ cm}^{-1}$

has a large gap between the two strips due to =NH<sub>2</sub> and =NH vibrating. This discrepancy at the end of the strip indicates the correct overlap between the intermolecular tensile forces and the atomic vibration that mentioned in previous studies [28, 29].

#### 4.4 SEM analysis

An SEM picture of LF-NPs is shown in Fig. 7, which obviously indicates the spherical NPs with an average diameter of about  $150\text{--}250\text{ nm}$ . The photograph clearly presents that no heterogeneity appears on the NPs surface.

#### 4.5 AFM measurement

Figure 8 shows the AFM images of optimized LF-NPs. The topography of 2D image shows moderately smooth surfaces with spherical shape, and 3D photo demonstrated that the NPs are synthesized in a uniform and homogeneous spectrum inside visible chains and valleys.

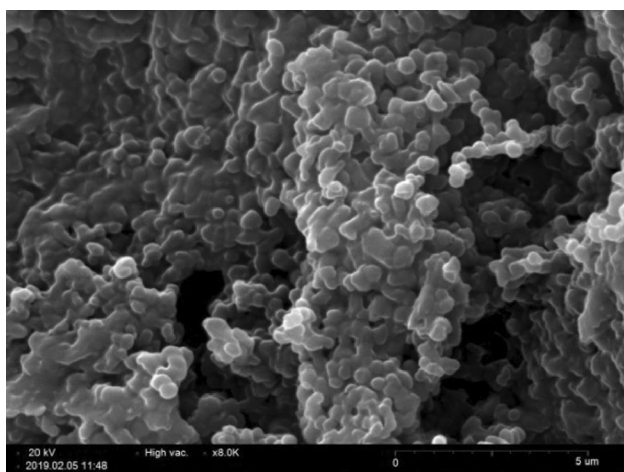


Fig. 7 SEM image of optimized LF-NPs

## 5 Conclusions

This study has shown that LF-NPs can be prepared by thermal treatment method. Physicochemical characterizations of the LF-NPs were estimated by FTIR, SEM and AFM analysis. Herein, Taguchi design method was applied to optimize the size of NPs. For this purpose, an L16 OA was arranged for the experiment procedure. From the ANOVA, found that LF concentration is most significant parameter for minimize the particle size of LF-NPs as compared to

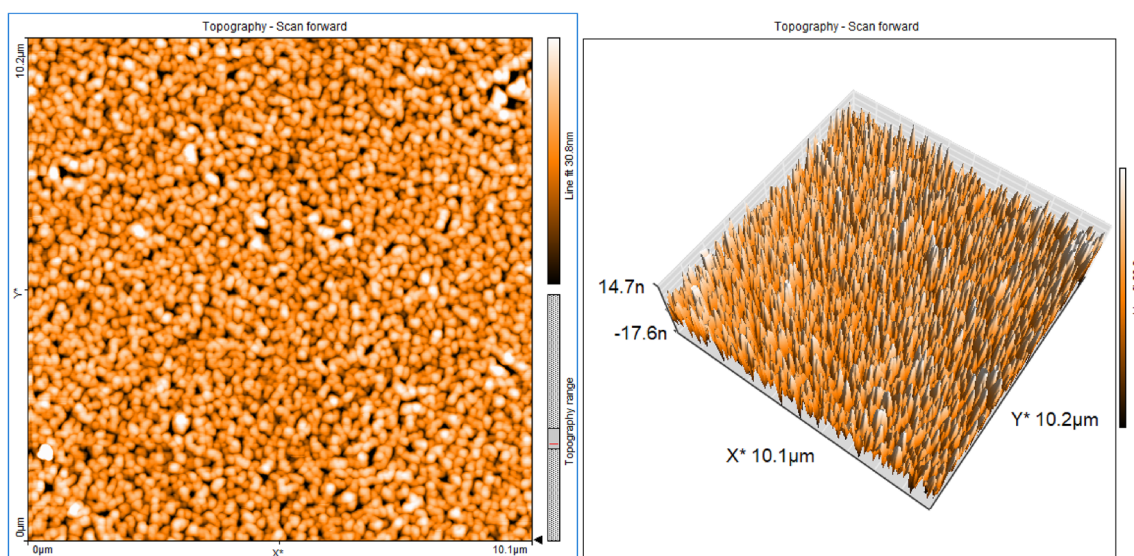


Fig. 8 AFM topography 2D and 3D images of optimized LF-NPs



others (contribution percentage ~ 45%). As a result, optimal conditions obtained of this method were: LF concentration of 3 mg/ml, pH 8, heating rate of 3 °C/min and final temperature of 90 °C to achieve minimum size equal to 188.8 nm which is in good agreement with data analyzed from Taguchi method (224.2 nm).

**Acknowledgements** This study was originally written as a part of Ph.D. thesis in chemical engineering. The authors would like to express their deepest thanks to Nanotechnology Research Institute, Babol Noshirovani University of Technology, for all their supports.

## Compliance with ethical standards

**Conflict of interest** The authors declare that they have no competing interests.

## References

- McLaren GD (2019) Iron deficiency. In: Lazarus H, Schmaier A (eds) Concise guide to hematology. Springer, Cham, pp 29–36. [https://doi.org/10.1007/978-3-319-97873-4\\_5](https://doi.org/10.1007/978-3-319-97873-4_5)
- Hashim HA, Foda O, Ghayaty E (2017) Lactoferrin or ferrous salts for iron deficiency anemia in pregnancy: a meta-analysis of randomized trials. *Eur J Obstet Gynecol Reprod Biol* 219:45–52
- Iglesias-Figueroa BF, Espinoza-Sánchez EA, Siqueiros-Cendón TS, Rascón-Cruz Q (2019) Lactoferrin as a nutraceutical protein from milk, an overview. *Int Dairy J* 89:37–41
- Liu L, Jiang R, Lönnerdal B (2019) Assessment of bioactivities of the human milk lactoferrin–osteopontin complex in vitro. *The Journal of nutritional biochemistry* 69:10–18
- Jenssen H, Hancock REW (2009) Antimicrobial properties of lactoferrin. *Biochimie* 91:19–29
- Locklin RM, Hulley PA, Naot D, Cornish J (2009) Lactoferrin protects osteoblasts and osteocytes from apoptosis. *Bone* 44:S317
- Zhang Y, Pu C, Tang W, Wang S, Sun Q (2019) Gallic acid liposomes decorated with lactoferrin: characterization, in vitro digestion and antibacterial activity. *Food Chem* 293:315–322
- Giansanti F, Leboffe L, Pitari G, Ippoliti R, Antonini G (2012) Physiological roles of ovotransferrin. *Biochim Biophys Acta BBA Gen Subj* 1820:218–225
- Bourbon AI, Martins JT, Pinheiro AC, Madalena DA, Marques A, Nunes R, Vicente AA (2019) Nanoparticles of lactoferrin for encapsulation of food ingredients. *Biopolym Nanostruct Food Encapsul Purp* 1:147–168
- Wakabayashi H, Oda H, Yamauchi K, Abe F (2014) Lactoferrin for prevention of common viral infections. *J Infect Chemother* 20:666–671
- Hassanzadeganroudsari M, Heydarinasab A, Chen P, Soltani M (2019) In vitro investigation of anticancer efficacy of carboplatin-loaded PEGylated nanoliposome particles on brain cancer cell lines. *J Nanopart Res* 21:124
- Roudsari MH, Saeidi N, Kabiri N, Ahmadi A, Tabrizi MM, Far ME, Shahmabadi HE, Khiyavi A, Reghbati B (2016) Investigation of characteristics and behavior of loaded carboplatin on the liposomes nanoparticles, on the lung and ovarian cancer: an in vitro evaluation. *Asian Pac J Cancer Biol* 1:9–12
- Shahavi MH, Najafpour GD, Jahanshahi M (2008) Hydrodynamic behaviour and biochemical characterization of a simple custom expanded bed column for protein purification. *Afr J Biotechnol* 7:4336–4344
- Li H, Tong Y, Bai L, Ye L, Zhong L, Duan X, Zhu Y (2018) Lactoferrin functionalized PEG-PLGA nanoparticles of shikonin for brain targeting therapy of glioma. *Int J Biol Macromol* 107:204–211
- Wang B, Timilsena YP, Blanch E, Adhikari B (2019) Lactoferrin: structure, function, denaturation and digestion. *Crit Rev Food Sci Nutr* 59:580–596
- Kumari S, Kondapi AK (2017) Lactoferrin nanoparticle mediated targeted delivery of 5-fluorouracil for enhanced therapeutic efficacy. *Int J Biol Macromol* 95:232–237
- Shahavi MH, Hosseini M, Jahanshahi M, Meyer RL, Darzi GN (2016) Clove oil nanoemulsion as an effective antibacterial agent: taguchi optimization method. *Desalin Water Treat* 57:18379–18390
- Shahidzadeh M, Shabih P, Pourmortazavi SM (2015) Sonochemical preparation of copper (II) chromite nanocatalysts and particle size optimization via taguchi method. *J Inorg Organomet Polym Mater* 25:986–994
- Shahavi MH, Hosseini M, Jahanshahi M, Meyer RL, Darzi GN (2015) Evaluation of critical parameters for preparation of stable clove oil nanoemulsion. *Arab J Chem*. <https://doi.org/10.1016/j.arabjc.2015.08.024>
- Boopathi S (2019) Experimental investigation and parameter analysis of LPG refrigeration system using Taguchi method. *SN Appl Sci* 1:892
- Bengoechea C, Peinado I, McClements DJ (2011) Formation of protein nanoparticles by controlled heat treatment of lactoferrin: factors affecting particle characteristics. *Food Hydrocoll* 25:1354–1360
- Ebrahimifar M, Nili-Ahmadabadi A, Akbarzadeh A, Shahmabadi HE, Hasanzadegan M, Moradi-Sardareh H, Madadzadeh H, Rezaee-diyari J (2017) Preparation, characterization and cytotoxic effects of pegylated nanoliposomal containing carboplatin on ovarian cancer cell lines. *Indian J Clin Biochem* 32:230–234
- Pérez Quiñones J, Brüggemann O, Kjemis J, Shahavi MH, Peniche Covas C (2018) Novel brassinosteroid-modified polyethylene glycol micelles for controlled release of agrochemicals. *J Agric Food Chem* 66:1612–1619
- Yang WHP, Tarng YS (1998) Design optimization of cutting parameters for turning operations based on the Taguchi method. *J Mater Process Technol* 84:122–129
- Duca G, Anghel L, Erhan RV (2018) Structural aspects of lactoferrin and serum transferrin observed by FTIR spectroscopy. *Chem J Mold* 13:111–116
- Barth A (2007) Infrared spectroscopy of proteins. *Biochim Biophys Acta (BBA) Bioenerg* 1767:1073–1101
- Tamm LK, Tatulian SA (1997) Infrared spectroscopy of proteins and peptides in lipid bilayers. *Q Rev Biophys* 30:365–429
- Saito Y, Iwata T (2012) Characterization of hydroxyl groups of highly crystalline  $\beta$ -chitin under static tension detected by FT-IR. *Carbohydr Polym* 87:2154–2159
- Jackson M, Mantsch HH (1991) Protein secondary structure from FT-IR spectroscopy: correlation with dihedral angles from three-dimensional Ramachandran plots. *Can J Chem* 69:1639–1642

**Publisher's Note** Springer Nature remains neutral with regard to jurisdictional claims in published maps and institutional affiliations.